

Sensitivity of the IceCube Upgrade to Atmospheric Neutrino Oscillations

The IceCube Collaboration

(a complete list of authors can be found at the end of the proceedings)

E-mail: philipp.eller@tum.de, kayla.leonard@icecube.wisc.edu,
jcw5951@psu.edu, rasmus.orsoe@tum.de

IceCube DeepCore, the existing low-energy extension of the IceCube Neutrino Observatory, was designed to lower the neutrino detection energy threshold to the GeV range. A new extension, called the IceCube Upgrade, will consist of seven additional strings installed within the DeepCore fiducial volume. The new modules will have spacings of about 20 m horizontally and 3 m vertically, compared to about 40-70 m horizontally and 7 m vertically in DeepCore. It will be deployed in the polar season of 2025/26. This additional hardware features new types of optical modules with multi-PMT configurations, as well as calibration devices. This upgrade will more than triple the number of PMT channels with respect to current IceCube, and will significantly enhance its capabilities in the GeV energy range. However, the increased channel count also poses new computational challenges for the event simulation, selection, and reconstruction. In this contribution we present updated oscillation sensitivities based on the latest advancements in simulation, event selection, and reconstruction techniques.

Corresponding authors: Philipp Eller^{1*}, Kayla Leonard DeHolton², Jan Weldert², Rasmus Ørsøe¹

¹ *Technical University of Munich, TUM School of Natural Sciences, Physics Department, 85747 Garching, Germany*

² *Dept. of Physics, Pennsylvania State University, University Park, PA 16802, USA*

* Presenter

The 38th International Cosmic Ray Conference (ICRC2023)
26 July – 3 August, 2023
Nagoya, Japan



1. Introduction

The IceCube Neutrino Observatory has been detecting atmospheric neutrinos in the GeV energy range using its low-energy extension DeepCore for the past decade [1, 2]. This data has been used to make precision measurements of the atmospheric neutrino oscillation parameters [3–5], tau neutrino appearance [4] and preference for the neutrino mass ordering (NMO) [6]. A new extension, called the IceCube Upgrade, will be deployed in the polar season of 2025/26 and will consist of seven additional strings installed within the DeepCore fiducial volume. The new modules will have spacings of about 20 m horizontally and 3 m vertically, compared to about 40-70 m horizontally and 7 m vertically in DeepCore. This additional hardware features new types of optical modules with multi-PMT configurations. DEggs consist of two 8-inch PMTs pointing up and downwards [7], while mDOMs consist of 24 3-inch PMTs pointing in all directions [8], as well as new calibration devices. This Upgrade will more than triple the number of PMT channels with respect to current IceCube, and will significantly enhance its capabilities in the GeV energy range.

The work presented here uses events simulated for the full 93-string detector configuration (“IC93”) using the state-of-the-art IceCube simulation chain, and new techniques that have been developed to clean the raw data, reconstruct events, and reject backgrounds (Sec. 2). We quantify the expected performance of the Upgrade detector extension, and compare to a scenario without the extension (Sec. 3). The sensitivities presented here supersede previous ones [9].

2. Simulation & Processing

2.1 Simulation

Events are simulated following a similar procedure to Ref. [5], including neutrino interactions with GENIE [10] and the two primary backgrounds (atmospheric muons and pure detector noise triggers), assuming our latest ice model which takes into account birefringence due to the crystalline structure of the ice [11]. For the IceCube and DeepCore strings, extra ice scattering and absorption in the refrozen boreholes is included due to different optical properties compared to the original glacial ice. For the Upgrade strings, the local ice property changes are not necessary because of a planned de-gassing procedure that will be used to eliminate air bubbles introduced in deployment. Event trigger and filtering is based on the current DeepCore implementation but adjusted to take into account the new multi-PMT Upgrade modules, delivering a realistic baseline performance, while further studies for optimized triggers and detector calibration with the new devices are ongoing.

2.2 Noise Cleaning

Radioactive decays in the glass housing of the optical modules are the largest source of noise pollution in the data. In the past, it has been sufficient to use cuts on the temporal and spatial distance of hits for noise cleaning. However, because of the increased channel count and the increased levels of radioactivity in the new modules’ glass, these cuts are no longer sufficient for the IceCube Upgrade. We developed a new cleaning algorithm based on a Graph Neural Network (GNN) specifically for the IceCube Upgrade. It performs a binary classification to predict whether a pulse is signal or noise. The GNN encodes the irregular grid of the detector and the irregular topology by representing each event as a point-cloud graph, where each node represents an observed

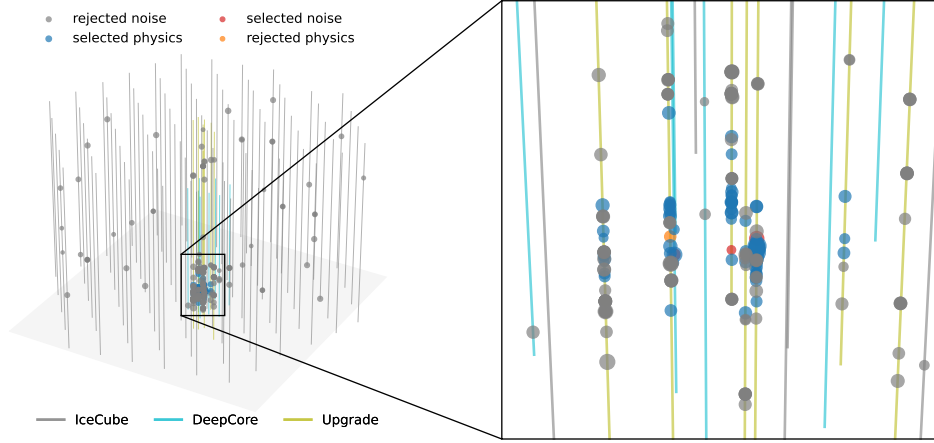


Figure 1: Event display of a 4.7 GeV muon neutrino interaction in the IceCube Upgrade. The existing IceCube and DeepCore strings are shown in grey and cyan, respectively, while the new IceCube Upgrade strings are shown in olive. This event has 96 hits caused by the neutrino interaction, of which 93 are correctly identified by the GNN (blue markers) and 3 are rejected (orange). The remaining 242 hits are caused by random detector noise: 240 are correctly rejected (grey) while 2 incorrectly pass the cleaning (red).

pulse in the detector and edges are drawn to the 8 nearest hits. For each node, we use features that describe the observed pulse such as charge and arrival time, and features that describe the PMT such as its position, relative optical efficiency, direction, and surface area.

We train a customized version of the GNN DynEdge [12] from the open-source framework *GraphNeT* [13], using a dataset with about 4 million neutrino and muon events. We apply a threshold of 0.7 on the classification output. An example event cleaned by the GNN is shown in Fig. 1. The GNN reduces the average amount of noise per neutrino event by a factor of about 10 with only a minor loss in signal. Before cleaning, 70% of hits in the uncleaned pulse series are noise, and after cleaning an average of 6.8% of noise hits remain. In addition, when the GNN is applied to pure noise events, less than 1% of these events survive. Neutrino events with at least 8 hits after cleaning on average retain 91% of the signal.

2.3 Reconstruction & Classification

After events are cleaned, four separate instances of DynEdge are trained to reconstruct and classify events based on the cleaned pulse series. These tasks include reconstructing the neutrino energy, zenith angle & uncertainty, and classifying events by particle type (muon vs. neutrino) and event topology (track vs. cascade). Each of the 4 models is trained on a different task-specific subsamples. Sample balancing is performed for the classification tasks. Figure 2 shows the reconstruction performance for energy and $\cos(\text{zenith})$. We find that the neutrino/muon classifier provides several orders of magnitude of background reduction. The track/cascade classifier achieves a 0.82 Area Under the Curve (AUC) score, which is a significant improvement compared to what's previously been reported for DynEdge for IC86 [12].

2.4 Event Selection

Several levels of cuts are used to suppress the main backgrounds (atmospheric muons and noise) and achieve a high-purity neutrino sample, summarized in Fig. 3. The first round con-

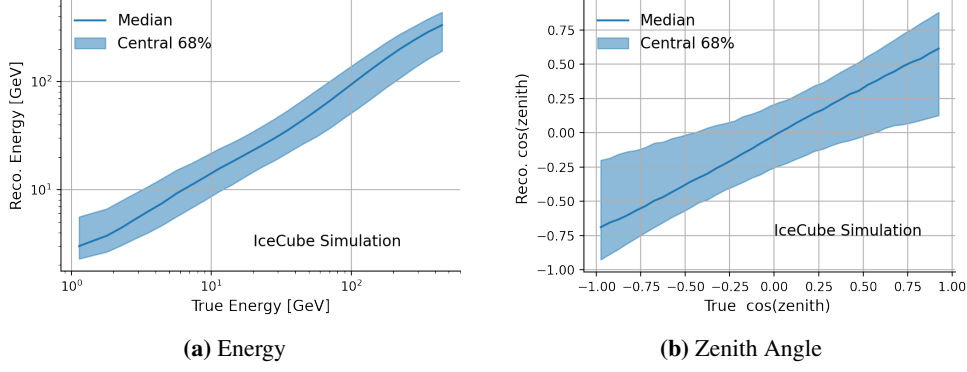


Figure 2: Performance for the reconstruction of neutrino energy (left) and zenith angle (right). Shown are the median and central 68% region of the reconstructed quantity as a function of the simulated truth. The bending of the angle towards the edges is due the quantity being bound $\in [-1, 1]$.

sists of a few simple straight cuts, similar to what was used in Ref. [5], that eliminate the most obvious background events. The cut with the largest rejection power is the number of pulses remaining after the noise cleaning procedure described above. After the straight cuts, a collection of machine learning classifiers are used to identify muon background events. One of these is the muon/neutrino GNN classifier described above. There are also two Boosted Decision Trees (BDTs) that use reconstructed quantities and variables describing the spatial and temporal distribution of the hits. These three classifiers are able to suppress the remaining muon background by three orders of magnitude resulting in a sample that is heavily dominated by neutrinos. A few final cuts are made to focus on the the events for which most of the oscillation signal comes from. Figure 4 shows the final level event distributions after these cuts are made.

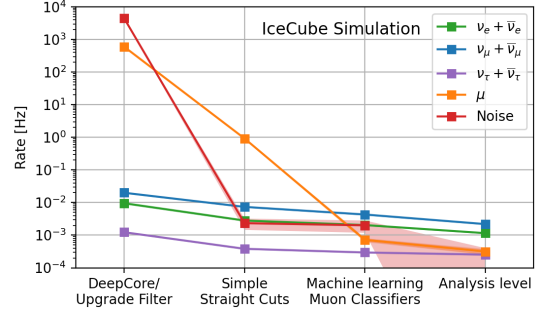


Figure 3: Event rates as a function of selection step, from filter level up to the analysis level.

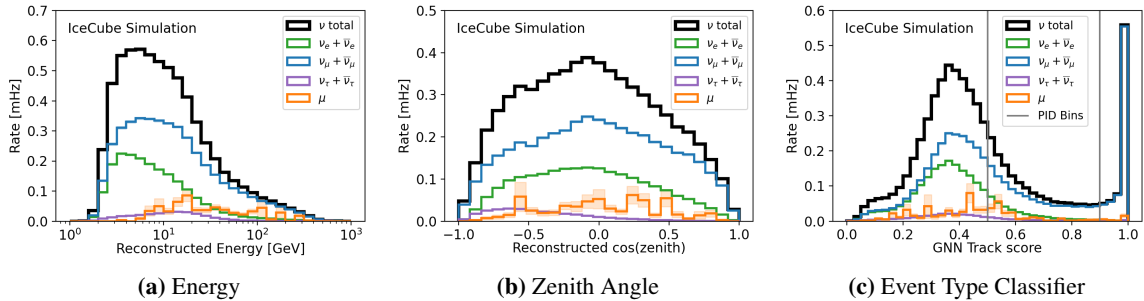


Figure 4: Distributions of final level event rates as a function of the three analysis observables. The shaded bands show 1σ statistical uncertainty, most visible for the muon background due to lower MC statistics.

3. Expected Oscillation Analysis Sensitivities

The analyses presented here largely follow previous DeepCore analyses, such as [5], and reflect realistic baseline sensitivities, while there is still room for improvement from better knowledge of systematic uncertainties and further optimization of the event selection and analysis choices. New, necessary parameters are added to take into account the new module types such as a new optical efficiency scale, and additional low energy cross section uncertainties are added since the energy threshold is lowered to 3 GeV. This leads to a different treatment for (simulated) data coming before and after the new strings are deployed. Therefore, the different time periods are treated as separate data sources and we run a combined, simultaneous fit with correlated parameters.

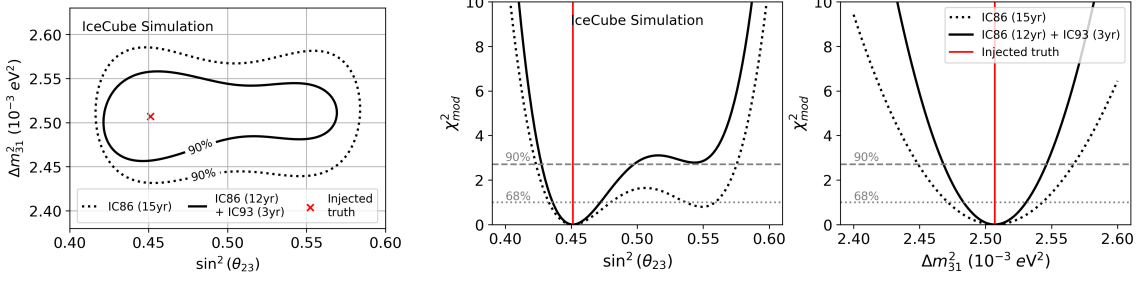
We present the IceCube sensitivities to the atmospheric oscillation parameters (Δm_{31}^2 and θ_{23}), a non-unitarity test with tau neutrinos, and the neutrino mass ordering. We compare two scenarios: one with no new hardware installed and data-taking continuing as it is today (denoted as “IC86”, reflecting the current 86 string detector). The other scenario includes the combined fit between 12 years of IC86 with additional years using the extra seven strings of the IceCube Upgrade from 2026 onwards (denoted as “IC86 (12 yr) + IC93”). Since the NMO signal is at a lower energy than the other analyses, different systematic uncertainties become more/less relevant, and therefore a slightly different set of parameters is used for the NMO analysis. An overview of the systematic uncertainties used is provided in Table 1, and more details on each can be found in Ref. [5]. The largest contributions to uncertainty are currently from flux parameters, though this can be improved in the future by switching to newer flux models with reduced uncertainty [14]. The analyses assume true normal ordering and oscillation parameter values from NuFit 5.2 [15].

Description	Parameter(s)	Atm. osc.	ν_τ	NMO
Flux				
Spectral index	γ	x	x	x
	d_π	-	-	x
Uncertainty on Pion and Kaon production (Barr et al. [16])	$g_\pi, h_\pi, i_\pi, w_K, z_K$	x	x	x
	y_K	x	x	-
Neutrino and Muon Normalizations	A_{eff}, μ_{atm}	x	x	x
Cross sections				
Deep inelastic scattering uncertainty [17]	DIS _{CSMS}	x	x	-
Axial masses for Resonant CC and Quasi-elastic scattering	$M_{A,res}^{CC}, M_{A,QE}$	x	x	x
Axial masses for Resonant NC and Coherent π scattering	$M_{A,res}^{NC}, M_{A,coh}$	-	-	x
Model uncertainty on tau neutrino cross section [18]	ν_τ xsec	-	-	x
Detector				
Bulk ice properties scattering and absorption	scat., abs.	x	x	x
Optical module efficiencies (IceCube and Upgrade modules)	$OM_{eff,ICDC}, OM_{eff,ICU}$	x	x	x
Angular acceptance (IC86 configuration only)	p_0, p_1	x	x	x
Oscillations				
Mixing Angles	θ_{13}	-	-	x
	θ_{23}	M	x	x
Mass splitting	Δm_{31}^2	M	x	x
Unitarity breaking parameter	ν_τ norm	-	M	-
Neutrino Mass Ordering	NMO	NO	NO	M

Table 1: Configuration of nuisance parameters for the analyses presented. The marker “x” indicates that a systematic is included in the fit, “-” means not included, and “M” denotes the measurement variable(s).

3.1 Atmospheric Oscillation Parameters

We follow a similar analysis procedure to existing IceCube measurements of the atmospheric oscillation parameters [5]. Figure 5a shows the sensitivity at the 90% confidence level after 3 years with the new strings. In Fig. 5b, one dimensional projections to the oscillation parameters are shown. The new strings increase IceCube’s sensitivity to Δm_{31}^2 and θ_{23} by about 20-30% and allow for a significantly better constraint of the atmospheric neutrino oscillation parameters.

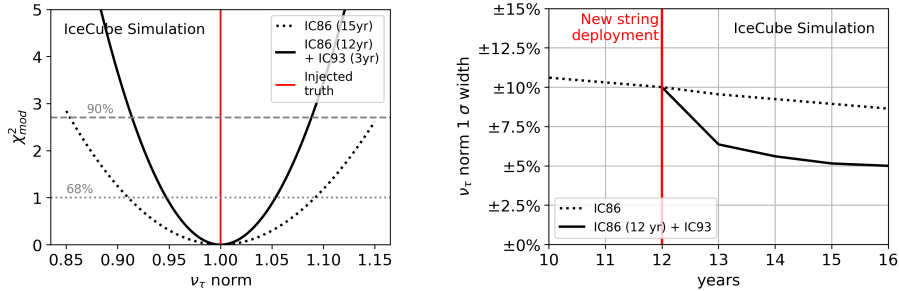


(a) Joint 90% CL sensitivity contours for the mixing angle θ_{23} and mass splitting Δm_{31}^2 . (b) One dimensional profile $\Delta\chi^2$ curves separately for both measurement parameters

Figure 5: Sensitivity contours and profiles, respectively, for the standard atmospheric mixing analysis. The solid black lines show the scenario where the IceCube Upgrade is in place, while the dashed lines show the performance without additional hardware. The assumed true value is indicated in red.

3.2 Non-unitary Mixing: Tau Neutrinos

This analysis shows how well we can constrain the unitarity of the PMNS matrix in the tau sector by scaling the amount of ν_τ appearance. More information about how IceCube measures ν_τ appearance can be found in [4]. Figure 6a compares the sensitivity to the ν_τ normalization with and without IceCube Upgrade. With the 3 years of data including Upgrade strings, the uncertainty can be almost reduced by a factor of two. To illustrate the evolution of this sensitivity, Fig. 6 shows the 1σ uncertainty on the ν_τ normalization as a function of the detector livetime. The new instrumentation will significantly improve IceCube’s ability to constrain this parameter.



(a) Profile $\Delta\chi^2$ curves for 15 years of livetime with and without including Upgrade (b) Width of the 1σ CL as a function of livetime

Figure 6: Sensitivity to the norm of the ν_τ unitarity breaking parameter for the scenario with DeepCore only (dashed line) and with the Upgrade included (solid lines).

3.3 Neutrino Mass Ordering

Finally, the sensitivity to the neutrino mass ordering is shown, where median sensitivity is defined according to [19]. More information about how IceCube determines the NMO can be found in [6]. Note that while the systematic parameters used for the NMO sensitivities were updated with respect to the previous two sections, however the other analysis choices are not fully optimized in the sensitivities presented below. IceCube’s sensitivity to the NMO strongly depends on the true value of θ_{23} ; Fig. 7 shows the sensitivity as a function of θ_{23} for both possible orderings separately. The sensitivity is significantly improved by adding the new strings. Figure 8 shows the evolution of the NMO sensitivity over time. With the additional strings, IceCube will reach more than 2σ within a few years for any allowed value of θ_{23} and either true ordering. Assuming a true normal ordering and preferential value of θ_{23} , more than 3σ sensitivities are expected within 5 years.

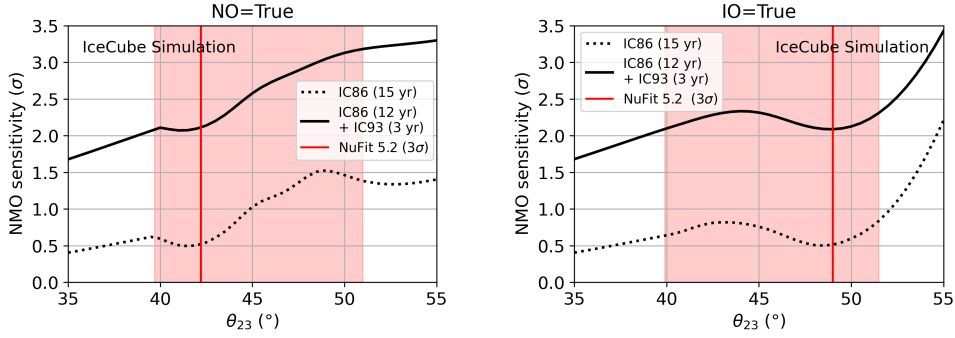


Figure 7: Sensitivity to the NMO as a function of θ_{23} for the scenario with DeepCore only (dashed line) and with the Upgrade included (solid lines). The left panel assumes a true NO, while the right panel assumes a true IO. The red line and band indicates the current NuFit best-fit value and $\pm 3\sigma$ uncertainty on θ_{23} .

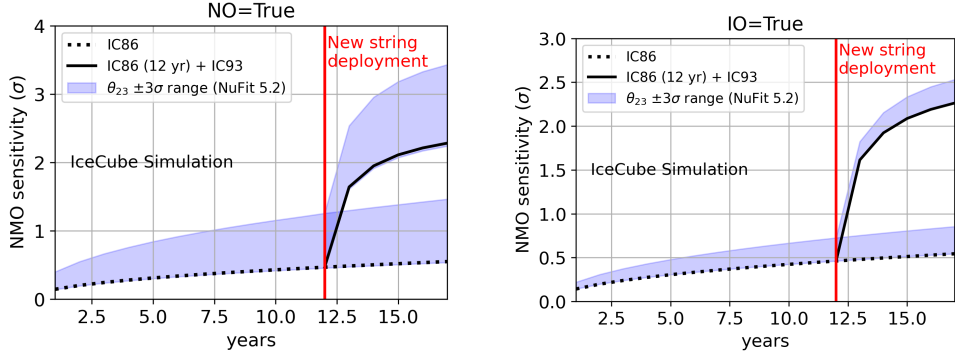


Figure 8: Sensitivity to the NMO as a function of livetime for the scenario with DeepCore only (dashed line) and with the Upgrade included (solid lines). The left panel assumes a true NO, while the right panel assumes a true IO. While the black lines assume the current best-fit value of θ_{23} by NuFit, the blue bands show the range of possible sensitivities within the $\pm 3\sigma$ uncertainty on θ_{23} .

4. Conclusions

In this work we presented the first end to end, full Monte Carlo based analysis for IceCube Upgrade oscillation physics, including new, realistic methods such as the GNN event cleaning and

reconstruction, as well as a new event selection pipeline. Strong improvements over the current IceCube DeepCore detector are expected. For a livetime of 3 years of the Upgrade detector, we expect to collect 315 thousand neutrinos with the selection presented here. This combined with the 277 thousand neutrinos expected from the 12 year data taken by IceCube DeepCore up until deployment, uncertainties are reduced at the order of 20-30% for the atmospheric neutrino oscillation parameters, around 40% for the tau normalization and a factor of almost 4× boost in NMO sensitivity is seen. The sensitivities presented are expected to improve in the future when leveraging the additional calibration devices that will be deployed with the Upgrade, and further optimizing the triggers, event selection & processing, and analysis choices.

References

- [1] **IceCube** Collaboration *JINST* **12** no. 03, (2017) P03012.
- [2] **IceCube** Collaboration *Astropart. Phys.* **35** (2012) 615–624.
- [3] **IceCube** Collaboration *Phys. Rev. Lett.* **120** no. 7, (2018) 071801.
- [4] **IceCube** Collaboration *Phys. Rev. D* **99** no. 3, (2019) 032007.
- [5] **IceCube Collaboration** Collaboration, R. Abbasi *et al.* *Phys. Rev. D* **108** (Jul, 2023) 012014.
- [6] **IceCube** Collaboration *Eur. Phys. J. C* **80** no. 1, (2020) 9.
- [7] **IceCube** Collaboration *JINST* **18** no. 04, (2023) P04014.
- [8] **IceCube** Collaboration *PoS ICRC2019* (2020) 855.
- [9] **IceCube** Collaboration *PoS ICRC2019* (2021) 1031.
- [10] C. Andreopoulos *et al.* *Nucl. Instrum. Meth. A* **614** (2010) 87–104.
- [11] M. Rongen and D. Chirkin on behalf of IceCube *JINST* **16** no. 09, (2021) C09014.
- [12] **IceCube** Collaboration *JINST* **17** no. 11, (2022) P11003.
- [13] A. Søggaard *et al.* *Journal of Open Source Software* **8** no. 85, (2023) 4971.
- [14] J. P. Yañez and A. Fedynitch. [arXiv:2303.00022](https://arxiv.org/abs/2303.00022) [hep-ph].
- [15] I. Esteban *et al.* *JHEP* **09** (2020) 178.
- [16] G. D. Barr *et al.* *Phys. Rev. D* **74** no. 9, (Nov, 2006) .
- [17] A. Gazizov and M. Kowalski *Computer Physics Communications* **172** no. 3, (2005) 203–213.
- [18] J. Conrad *et al.* *Phys. Rev. D* **82** (2010) 093012.
- [19] M. Blennow *et al.* *JHEP* **03** (2014) 028.

Full Author List: IceCube Collaboration

R. Abbasi¹⁷, M. Ackermann⁶³, J. Adams¹⁸, S. K. Agarwalla^{40, 64}, J. A. Aguilar¹², M. Ahlers²², J.M. Alameddine²³, N. M. Amin⁴⁴, K. Andeen⁴², G. Anton²⁶, C. Argüelles¹⁴, Y. Ashida⁵³, S. Athanasiadou⁶³, S. N. Axani⁴⁴, X. Bai⁵⁰, A. Balagopal V.⁴⁰, M. Baricevic⁴⁰, S. W. Barwick³⁰, V. Basu⁴⁰, R. Bay⁸, J. J. Beatty^{20, 21}, J. Becker Tjus^{11, 65}, J. Beise⁶¹, C. Bellenghi²⁷, C. Benning¹, S. BenZvi⁵², D. Berley¹⁹, E. Bernardini⁴⁸, D. Z. Besson³⁶, E. Blaufuss¹⁹, S. Blot⁶³, F. Bontempo³¹, J. Y. Book¹⁴, C. Boscolo Meneguolo⁴⁸, S. Böser⁴¹, O. Botner⁶¹, J. Böttcher⁷, E. Bourbeau²², J. Braun⁴⁰, B. Brinson⁶, J. Brostean-Kaiser⁶³, R. T. Burley², R. S. Busse⁴³, D. Butterfield⁴⁰, M. A. Campana⁴⁹, K. Carloni¹⁴, E. G. Carnie-Bronca², S. Chattopadhyay^{40, 64}, N. Chau¹², C. Chen⁶, Z. Chen⁵⁵, D. Chirkin⁴⁰, S. Choi⁵⁶, B. A. Clark¹⁹, L. Classen⁴³, A. Coleman⁶¹, G. H. Collin¹⁵, A. Connolly^{20, 21}, J. M. Conrad¹⁵, P. Coppin¹³, P. Correa¹³, D. F. Cowen^{59, 60}, P. Dave⁶, C. De Clercq¹³, J. J. DeLaunay⁵⁸, D. Delgado¹⁴, S. Deng¹, K. Deoskar⁵⁴, A. Desai⁴⁰, P. Desati⁴⁰, K. D. de Vries¹³, G. de Wasseige³⁷, T. DeYoung²⁴, A. Diaz¹⁵, J. C. Díaz-Vélez⁴⁰, M. Dittmer⁴³, A. Domi²⁶, H. Dujmovic⁴⁰, M. A. DuVernois⁴⁰, T. Ehrhardt⁴¹, P. Eller²⁷, E. Ellinger⁶², S. El Mentawi¹, D. Elsässer²³, R. Engel^{31, 32}, H. Erpenbeck⁴⁰, J. Evans¹⁹, P. A. Evenson⁴⁴, K. L. Fan¹⁹, K. Fang⁴⁰, K. Farrag¹⁶, A. R. Fazley⁷, A. Fedynitch⁵⁷, N. Feigl¹⁰, S. Fiedlschuster²⁶, C. Finley⁵⁴, L. Fischer⁴⁰, D. Fox⁵⁹, A. Frankowiak¹¹, A. Fritz⁴¹, P. Fürst¹, J. Gallagher³⁹, E. Ganster¹, A. Garcia¹⁴, L. Gerhardt⁹, A. Ghadimi⁵⁸, C. Glaser⁶¹, T. Glauch²⁷, T. Glusenkamp^{26, 61}, N. Goehke³², J. G. Gonzalez⁴⁴, S. Goswami⁵⁸, D. Grant²⁴, S. J. Gray¹⁹, O. Gries¹, S. Griffin⁴⁰, S. Griswold⁵², K. M. Groth²², C. Günther¹, P. Gutjahr²³, C. Haack²⁶, A. Hallgren⁶¹, R. Halliday²⁴, L. Halve¹, F. Halzen⁴⁰, H. Hamdaoui⁵⁵, M. Ha Minh²⁷, K. Hanson⁴⁰, J. Hardin¹⁵, A. A. Harnisch²⁴, P. Hatch³³, A. Haungs³¹, K. Helbing⁶², J. Hellrung¹¹, F. Henningsen²⁷, L. Heuermann¹, N. Heyer⁶¹, S. Hickford⁶², A. Hidvegi⁵⁴, C. Hill¹⁶, G. C. Hill², K. D. Hoffman¹⁹, S. Hori⁴⁰, K. Hoshina^{40, 66}, W. Hou³¹, T. Huber³¹, K. Hultqvist²³, M. Hünnefeld²³, R. Hussain⁴⁰, K. Hymon²³, S. In⁵⁶, A. Ishihara¹⁶, M. Jacquart⁴⁰, O. Janik¹, M. Jansson⁵⁴, G. S. Japaridze⁵, M. Jeong⁵⁶, M. Jin¹⁴, B. J. P. Jones⁴, D. Kang³¹, W. Kang⁵⁶, X. Kang⁴⁹, A. Kappes⁴³, D. Kappesser⁴¹, L. Kardum²³, T. Karg⁶³, M. Karle²⁷, A. Karle⁴⁰, U. Katz²⁶, M. Kauer⁴⁰, J. L. Kelley⁴⁰, A. Khatee Zathul⁴⁰, A. Kheirandish^{34, 35}, J. Kiryluk⁵⁵, S. R. Klein^{8, 9}, A. Kochocki²⁴, R. Koirala⁴⁴, H. Kolanoski¹⁰, T. Kontrimas²⁷, L. Köpke⁴¹, C. Kopper²⁶, D. J. Koskinen²², P. Koundal³¹, M. Kovacevich⁴⁹, M. Kowalski^{10, 63}, T. Kozynets²², J. Krishnamoorthi^{40, 64}, K. Kruiswijk³⁷, E. Krupczak²⁴, A. Kumar⁶³, E. Kun¹¹, N. Kurahashi⁴⁹, N. Lad⁶³, C. Lagunas Gualda⁶³, M. Lamoureux³⁷, M. J. Larson¹⁹, S. Latseva¹, F. Lauber⁶², J. P. Lazar^{14, 40}, J. W. Lee⁵⁶, K. Leonard DeHolton⁶⁰, A. Leszczyńska⁴⁴, M. Lincetto¹¹, Q. R. Liu⁴⁰, M. Liubarska²⁵, E. Lohfink⁴¹, C. Love⁴⁹, C. J. Lozano Mariscal⁴³, L. Lu⁴⁰, F. Lucarelli²⁸, W. Luszczak^{20, 21}, Y. Lyu^{8, 9}, J. Madsen⁴⁰, K. B. M. Mahn²⁴, Y. Makino⁴⁰, E. Manao²⁷, S. Mancina^{40, 48}, W. Marie Sainte⁴⁰, I. C. Mariş¹², S. Marka⁴⁶, Z. Marka⁴⁶, M. Marsee⁵⁸, I. Martinez-Soler¹⁴, R. Maruyama⁴⁵, F. Mayhew²⁴, T. McElroy²⁵, F. McNally³⁸, J. V. Mead²², K. Meagher⁴⁰, S. Mechbal⁶³, A. Medina²¹, M. Meier¹⁶, Y. Merckx¹³, L. Merten¹¹, J. Micallef²⁴, J. Mitchell⁷, T. Montaruli²⁸, R. W. Moore²⁵, Y. Morii¹⁶, R. Morse⁴⁰, M. Moulai⁴⁰, T. Mukherjee³¹, R. Naab⁶³, R. Nagai¹⁶, M. Nakos⁴⁰, U. Naumann⁶², J. Necker⁶³, A. Negi⁴, M. Neumann⁴³, H. Niederhausen²⁴, M. U. Nisa²⁴, A. Noell¹, A. Novikov⁴⁴, S. C. Nowicki²⁴, A. Obertacke Pollmann¹⁶, V. O'Dell⁴⁰, M. Oehler³¹, B. Oeyen²⁹, A. Olivas¹⁹, R. Ørsøe²⁷, J. Osborn⁴⁰, E. O'Sullivan⁶¹, H. Pandya⁴⁴, N. Park³³, G. K. Parker⁴, E. N. Paudel⁴⁴, L. Paul^{42, 50}, C. Pérez de los Heros⁶¹, J. Peterson⁴⁰, S. Philippen¹, A. Pizzuto⁴⁰, M. Plum⁵⁰, A. Pontén⁶¹, Y. Popovych⁴¹, M. Prado Rodriguez⁴⁰, B. Pries²⁴, R. Procter-Murphy¹⁹, G. T. Przybylski⁹, C. Raab³⁷, J. Rack-Helleis⁴¹, K. Rawlins³, Z. Rechav⁴⁰, A. Rehman⁴⁴, P. Reichherzer¹¹, G. Renzi¹², E. Resconi²⁷, S. Reusch⁶³, W. Rhode²³, B. Riedel⁴⁰, A. Rifaie¹, E. J. Roberts², S. Robertson^{8, 9}, S. Rodan⁵⁶, G. Roellinghoff⁵⁶, M. Rongen²⁶, C. Rott^{53, 56}, T. Ruhe²³, L. Ruohan²⁷, D. Ryckbosch²⁹, I. Safa^{14, 40}, J. Saffer³², D. Salazar-Gallegos²⁴, P. Sampathkumar³¹, S. E. Sanchez Herrera²⁴, A. Sandrock⁶², M. Santander⁵⁸, S. Sarkar²⁵, S. Sarkar⁴⁷, J. Savelberg¹, P. Savina⁴⁰, M. Schaufel¹, H. Schieler³¹, S. Schindler²⁶, L. Schlickmann¹, B. Schlüter⁴³, F. Schlüter¹², N. Schmeisser⁶², T. Schmidt¹⁹, J. Schneider²⁶, F. G. Schröder^{31, 44}, L. Schumacher²⁶, G. Schwefer¹, S. Sclafani¹⁹, D. Seckel⁴⁴, M. Seikh³⁶, S. Seunarine⁵¹, R. Shah⁴⁹, A. Sharma⁶¹, S. Shefali³², N. Shimizu¹⁶, M. Silva⁴⁰, B. Skrzypek¹⁴, B. Smithers⁴, R. Snihur⁴⁰, J. Soedingrekso²³, A. Sogaard²², D. Soldin³², P. Soldin¹, G. Sommani¹¹, C. Spannfellner²⁷, G. M. Spiczak⁵¹, C. Spiering⁶³, M. Stamatikos²¹, T. Stanev⁴⁴, T. Stetzelberger⁹, T. Stürwald⁶², T. Stuttard²², G. W. Sullivan¹⁹, I. Taboada⁶, S. Ter-Antonyan⁷, M. Thiesmeyer¹, W. G. Thompson¹⁴, J. Thwaites⁴⁰, S. Tilav⁴⁴, K. Tollefson²⁴, C. Tönnis⁵⁶, S. Toscano¹², D. Tosi⁴⁰, A. Trettin⁶³, C. F. Tung⁶, R. Turcotte³¹, J. P. Twagirayezu²⁴, B. Ty⁴⁰, M. A. Unland Elorrieta⁴³, A. K. Upadhyay^{40, 64}, K. Upshaw⁷, N. Valtonen-Mattila⁶¹, J. Vandenbroucke⁴⁰, N. van Eijndhoven¹³, D. Vannerom¹⁵, J. van Santen⁶³, J. Vara⁴³, J. Veitch-Michaelis⁴⁰, M. Venugopal³¹, M. Vereecken³⁷, S. Verpoest⁴⁴, D. Veske⁴⁶, A. Vijai¹⁹, C. Walck⁵⁴, C. Weaver²⁴, P. Weigel¹⁵, A. Weindl³¹, J. Weldert⁶⁰, C. Wendt⁴⁰, J. Werthebach²³, M. Weyrauch³¹, N. Whitehorn²⁴, C. H. Wiebusch¹, N. Willey²⁴, D. R. Williams⁵⁸, L. Witthaus²³, A. Wolf¹, M. Wolf²⁷, G. Wrede²⁶, X. W. Xu⁷, J. P. Yanez²⁵, E. Yildizci⁴⁰, S. Yoshida¹⁶, R. Young³⁶, F. Yu¹⁴, S. Yu²⁴, T. Yuan⁴⁰, Z. Zhang⁵⁵, P. Zhelnin¹⁴, M. Zimmerman⁴⁰

¹ III. Physikalisches Institut, RWTH Aachen University, D-52056 Aachen, Germany

² Department of Physics, University of Adelaide, Adelaide, 5005, Australia

³ Dept. of Physics and Astronomy, University of Alaska Anchorage, 3211 Providence Dr., Anchorage, AK 99508, USA

⁴ Dept. of Physics, University of Texas at Arlington, 502 Yates St., Science Hall Rm 108, Box 19059, Arlington, TX 76019, USA

⁵ CTSPS, Clark-Atlanta University, Atlanta, GA 30314, USA

⁶ School of Physics and Center for Relativistic Astrophysics, Georgia Institute of Technology, Atlanta, GA 30332, USA

⁷ Dept. of Physics, Southern University, Baton Rouge, LA 70813, USA

⁸ Dept. of Physics, University of California, Berkeley, CA 94720, USA

⁹ Lawrence Berkeley National Laboratory, Berkeley, CA 94720, USA

¹⁰ Institut für Physik, Humboldt-Universität zu Berlin, D-12489 Berlin, Germany

¹¹ Fakultät für Physik & Astronomie, Ruhr-Universität Bochum, D-44780 Bochum, Germany

¹² Université Libre de Bruxelles, Science Faculty CP230, B-1050 Brussels, Belgium

- ¹³ Vrije Universiteit Brussel (VUB), Dienst ELEM, B-1050 Brussels, Belgium
- ¹⁴ Department of Physics and Laboratory for Particle Physics and Cosmology, Harvard University, Cambridge, MA 02138, USA
- ¹⁵ Dept. of Physics, Massachusetts Institute of Technology, Cambridge, MA 02139, USA
- ¹⁶ Dept. of Physics and The International Center for Hadron Astrophysics, Chiba University, Chiba 263-8522, Japan
- ¹⁷ Department of Physics, Loyola University Chicago, Chicago, IL 60660, USA
- ¹⁸ Dept. of Physics and Astronomy, University of Canterbury, Private Bag 4800, Christchurch, New Zealand
- ¹⁹ Dept. of Physics, University of Maryland, College Park, MD 20742, USA
- ²⁰ Dept. of Astronomy, Ohio State University, Columbus, OH 43210, USA
- ²¹ Dept. of Physics and Center for Cosmology and Astro-Particle Physics, Ohio State University, Columbus, OH 43210, USA
- ²² Niels Bohr Institute, University of Copenhagen, DK-2100 Copenhagen, Denmark
- ²³ Dept. of Physics, TU Dortmund University, D-44221 Dortmund, Germany
- ²⁴ Dept. of Physics and Astronomy, Michigan State University, East Lansing, MI 48824, USA
- ²⁵ Dept. of Physics, University of Alberta, Edmonton, Alberta, Canada T6G 2E1
- ²⁶ Erlangen Centre for Astroparticle Physics, Friedrich-Alexander-Universität Erlangen-Nürnberg, D-91058 Erlangen, Germany
- ²⁷ Technical University of Munich, TUM School of Natural Sciences, Department of Physics, D-85748 Garching bei München, Germany
- ²⁸ Département de physique nucléaire et corpusculaire, Université de Genève, CH-1211 Genève, Switzerland
- ²⁹ Dept. of Physics and Astronomy, University of Gent, B-9000 Gent, Belgium
- ³⁰ Dept. of Physics and Astronomy, University of California, Irvine, CA 92697, USA
- ³¹ Karlsruhe Institute of Technology, Institute for Astroparticle Physics, D-76021 Karlsruhe, Germany
- ³² Karlsruhe Institute of Technology, Institute of Experimental Particle Physics, D-76021 Karlsruhe, Germany
- ³³ Dept. of Physics, Engineering Physics, and Astronomy, Queen's University, Kingston, ON K7L 3N6, Canada
- ³⁴ Department of Physics & Astronomy, University of Nevada, Las Vegas, NV, 89154, USA
- ³⁵ Nevada Center for Astrophysics, University of Nevada, Las Vegas, NV 89154, USA
- ³⁶ Dept. of Physics and Astronomy, University of Kansas, Lawrence, KS 66045, USA
- ³⁷ Centre for Cosmology, Particle Physics and Phenomenology - CP3, Université catholique de Louvain, Louvain-la-Neuve, Belgium
- ³⁸ Department of Physics, Mercer University, Macon, GA 31207-0001, USA
- ³⁹ Dept. of Astronomy, University of Wisconsin–Madison, Madison, WI 53706, USA
- ⁴⁰ Dept. of Physics and Wisconsin IceCube Particle Astrophysics Center, University of Wisconsin–Madison, Madison, WI 53706, USA
- ⁴¹ Institute of Physics, University of Mainz, Staudinger Weg 7, D-55099 Mainz, Germany
- ⁴² Department of Physics, Marquette University, Milwaukee, WI, 53201, USA
- ⁴³ Institut für Kernphysik, Westfälische Wilhelms-Universität Münster, D-48149 Münster, Germany
- ⁴⁴ Bartol Research Institute and Dept. of Physics and Astronomy, University of Delaware, Newark, DE 19716, USA
- ⁴⁵ Dept. of Physics, Yale University, New Haven, CT 06520, USA
- ⁴⁶ Columbia Astrophysics and Nevis Laboratories, Columbia University, New York, NY 10027, USA
- ⁴⁷ Dept. of Physics, University of Oxford, Parks Road, Oxford OX1 3PU, United Kingdom
- ⁴⁸ Dipartimento di Fisica e Astronomia Galileo Galilei, Università Degli Studi di Padova, 35122 Padova PD, Italy
- ⁴⁹ Dept. of Physics, Drexel University, 3141 Chestnut Street, Philadelphia, PA 19104, USA
- ⁵⁰ Physics Department, South Dakota School of Mines and Technology, Rapid City, SD 57701, USA
- ⁵¹ Dept. of Physics, University of Wisconsin, River Falls, WI 54022, USA
- ⁵² Dept. of Physics and Astronomy, University of Rochester, Rochester, NY 14627, USA
- ⁵³ Department of Physics and Astronomy, University of Utah, Salt Lake City, UT 84112, USA
- ⁵⁴ Oskar Klein Centre and Dept. of Physics, Stockholm University, SE-10691 Stockholm, Sweden
- ⁵⁵ Dept. of Physics and Astronomy, Stony Brook University, Stony Brook, NY 11794-3800, USA
- ⁵⁶ Dept. of Physics, Sungkyunkwan University, Suwon 16419, Korea
- ⁵⁷ Institute of Physics, Academia Sinica, Taipei, 11529, Taiwan
- ⁵⁸ Dept. of Physics and Astronomy, University of Alabama, Tuscaloosa, AL 35487, USA
- ⁵⁹ Dept. of Astronomy and Astrophysics, Pennsylvania State University, University Park, PA 16802, USA
- ⁶⁰ Dept. of Physics, Pennsylvania State University, University Park, PA 16802, USA
- ⁶¹ Dept. of Physics and Astronomy, Uppsala University, Box 516, S-75120 Uppsala, Sweden
- ⁶² Dept. of Physics, University of Wuppertal, D-42119 Wuppertal, Germany
- ⁶³ Deutsches Elektronen-Synchrotron DESY, Platanenallee 6, 15738 Zeuthen, Germany
- ⁶⁴ Institute of Physics, Sachivalaya Marg, Sainik School Post, Bhubaneswar 751005, India
- ⁶⁵ Department of Space, Earth and Environment, Chalmers University of Technology, 412 96 Gothenburg, Sweden
- ⁶⁶ Earthquake Research Institute, University of Tokyo, Bunkyo, Tokyo 113-0032, Japan

Acknowledgements

The authors gratefully acknowledge the support from the following agencies and institutions: USA – U.S. National Science Foundation-Office of Polar Programs, U.S. National Science Foundation-Physics Division, U.S. National Science Foundation-EPSCoR, Wisconsin Alumni Research Foundation, Center for High Throughput Computing (CHTC) at the University of Wisconsin–Madison, Open Science

Grid (OSG), Advanced Cyberinfrastructure Coordination Ecosystem: Services & Support (ACCESS), Frontera computing project at the Texas Advanced Computing Center, U.S. Department of Energy-National Energy Research Scientific Computing Center, Particle astrophysics research computing center at the University of Maryland, Institute for Cyber-Enabled Research at Michigan State University, and Astroparticle physics computational facility at Marquette University; Belgium – Funds for Scientific Research (FRS-FNRS and FWO), FWO Odysseus and Big Science programmes, and Belgian Federal Science Policy Office (Belspo); Germany – Bundesministerium für Bildung und Forschung (BMBF), Deutsche Forschungsgemeinschaft (DFG), Helmholtz Alliance for Astroparticle Physics (HAP), Initiative and Networking Fund of the Helmholtz Association, Deutsches Elektronen Synchrotron (DESY), and High Performance Computing cluster of the RWTH Aachen; Sweden – Swedish Research Council, Swedish Polar Research Secretariat, Swedish National Infrastructure for Computing (SNIC), and Knut and Alice Wallenberg Foundation; European Union – EGI Advanced Computing for research; Australia – Australian Research Council; Canada – Natural Sciences and Engineering Research Council of Canada, Calcul Québec, Compute Ontario, Canada Foundation for Innovation, WestGrid, and Compute Canada; Denmark – Villum Fonden, Carlsberg Foundation, and European Commission; New Zealand – Marsden Fund; Japan – Japan Society for Promotion of Science (JSPS) and Institute for Global Prominent Research (IGPR) of Chiba University; Korea – National Research Foundation of Korea (NRF); Switzerland – Swiss National Science Foundation (SNSF); United Kingdom – Department of Physics, University of Oxford.